J Mater Sci (2007) 42:9181–9186
DOI 10.1007/s10853-007-1923-0

Synthesis and characterization of copper sulfide nanocrystal with three-dimensional flower-shape

Jing Zou · Jianxue Zhang · Baohua Zhang · Pingtang Zhao · Xiaofeng Xu · Jun Chen · Kaixun Huang

Received: 12 December 2006 / Accepted: 6 June 2007 / Published online: 27 July 2007

Abstract New copper sulfide nanocrystals with three-dimensional (3D) flower-shape were synthesized by using copper acetate ($Cu(ac)_2$) and citric acid (cit) and thiourea (Tu) as precursors at 160 °C in an anhydrous ethanol by a solvothermal route. The structure and properties of as-prepared products were characterized by X-ray powder diffraction, transmission electron microscopy, field emission scanning electron microscope and scanning electron microscope. The optical properties of copper sulfide nanocrystals were examined by UV–vis and FTIR. The crystal growth mechanism was also proposed.

Introduction

Design of new nanobuilding blocks and architectural control synthesis of nanocrystals with well-defined morphology in superstructure materials have attracted significant interest of chemist and material scientist, because of their unique optical, electrical and catalytic properties that rely sensitively on both size and shape of the samples are completely distinct from the bulk materials [1, 2].

For the past few years, various efforts have been made to control the architecture and spatial patterning of metal chalcogenide semiconductor particles. Copper sulfide is a good prospective optoelectronic material. It has potential applications in solar cells, electrochemistry cells, IR detectors, sensors, and catalysts [3–13]. For these applications, a variety of techniques [14–21] have been developed to prepare copper sulfides with controllable microstructural morphologies such as nanoparticles, hollow spheres, flakes, rods, wires, belt or flowerlike structures [22–27]. However, copper sulfide has very complex crystal chemistry owing to its ability to form various stoichiometric compounds. Mixture phase copper sulfides are usually obtained in many synthetic routes.

In this paper, a new solution approach to synthesize well-defined morphology of CuS nanocrystals with 3D flowerlike at low temperatures by a simple solvothermal process in anhydrous ethanol was reported. These CuS nanocrystals with 3D flower-shape were assembled by thin uniform single-crystalline nanosheets with thickness of ~3–6 nm and showed very strong UV bandage and IR absorption.

Experiment

For all the reactions in this study, the mixture of copper acetate monohydrate $(Cu(ac)_2) \cdot H_2O$ and citric acid (cit) was used as Cu sources, thiourea (Tu) (H_2NCSNH_2) was used as sulfur sources, respectively. In a typical process, the reactant molar ratio (C_R) of Tu:$Cu(ac)_2$, 2 mmol $Cu(ac)_2$ and 4 mmol cit was dissolved in 40 mL anhydrous ethanol; in another container, 6 mmol Tu was dissolved in 40 mL anhydrous ethanol. The Cu solution was added to the thiourea solution dropwise at room temperature with continuous stirring for 30 min. Then the mixture was transferred into a 100 mL Teflon-lied autoclave for solvothermal processing at 160 °C for 8 h in an electric

J. Zou · P. Zhao · K. Huang (✉)
Department of Chemistry, Huazhong University of Science and Technology, Wuhan, Hubei 430074, P.R. China
e-mail: hxxzrf@mail.hust.edu.cn

J. Zou · J. Zhang · B. Zhang · X. Xu · J. Chen
School of Chemical Engineering and Pharmacy, Wuhan Institute of Technology, Wuhan, Hubei 430074, P.R. China

desiccation box. After this process, black crystalline products were collected by centrifugation and thorough washings with water and ethanol for several times then dried at 50 °C in air for 4 h. The X-ray powder diffraction (XRD) pattern of the samples was characterized using a Japan XD-5A X-ray diffractometer with Cu Kα radiation (λ = 1.5406 Å) and a scanning rate of 0.08 degree/s in 2θ ranges from 15° to 70°; EDX spectrum was recorded at EDAX-FALCON60; scanning electron microscope (SEM) and field emission scanning electron microscope (FESEM) was carried out on a JEOL JSM-5510LV and a FEI Sirion 200, respectively. The powder samples were dispersed into ethanol and then placed on the copper wafers for SEM and FESEM observation. Transmission electron microscopy (TEM) images and selected-area electron diffraction (SAED) patterns were obtained by a transmission electron microscope (JEOL JEM-2010) with an accelerating voltage of 200 kV. A drop of the solution was dried on a holey copper grid for TEM and SAED observation. The optical property tests of the samples were carried out on a HP-8452A UV–vis absorption spectrometer and FTIR absorption spectrometer from Nicolet Impact 420.

Results and discussion

Figure 1 shows a typical XRD pattern of as-prepared CuS nanocrystals. All the reflections could be indexed to the pure hexagonal CuS in a good agreement with the reported data (JCPDS 06-0464; a = 3.791, c = 16.34). No impurities could be detected in this pattern, which implies that pure CuS could be obtained under the current synthetic route. The strong relative intensity of the [107] peak indicated preferentially orientation effects of the growth direction of nanosheet of hexagonal copper sulfide [19].

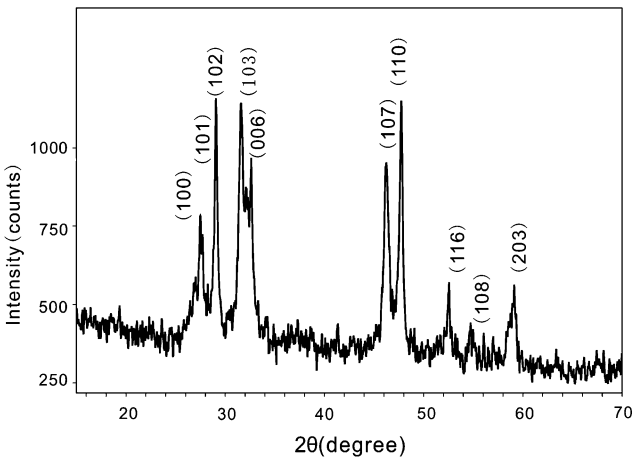

Fig. 1 Powder X-ray diffraction pattern (XRD) of as-prepared copper sulfide products

The EDX result (Fig. 2) demonstrates two elements of only Cu and S contained in the sample; the Cu:S atomic ratio was determined to be 1:1, suggesting that pure copper sulfide was fabricated.

Figure 3a shows a typical SEM image of CuS nanocrystals obtained by the solvothermal route via 2 mmol $Cu(ac)_2$ and 4 mmol cit solution reacting with 6 mmol Tu solution at 160 °C for 8 h. Perfect CuS nanocrystals with 3D flower-shape were assembled by many ultrathin and uniform nanosheets. Careful examination reveals that these CuS nanosheets are 3–6 nm in thickness and CuS nanoflowers are 2–5 μm in diameter. The products were further characterized by TEM (Fig. 3b). The corresponding SAED pattern (inset Fig. 3b) exhibits polycrystalline rings of copper sulfide. To give a further understanding of these flowers assembled, the samples were intensively sonicated for 20 min in ethanol. Many individual petal and residual CuS nanoflowers could be found in the sonicated sample. The TEM image of a residual CuS nanoflower and typical copper sulfide sheet after sonication is shown in Fig. 3c. The corresponding SAED pattern (inset Fig. 3c) implies that the individual nanoslice is single crystals with pure hexagonal copper sulfide. This verifies further that perfect CuS nanocrystals with 3D flower-shape are assembled by many spokewise single-crystalline nanostructured sheets.

It was reported that many factors had significant effects on the shapes and sizes of the halcogenide nanocrystals in previous studies [28, 29]. In this study, five major factors including the reactant molar ratio (C_R) of Tu:$Cu(ac)_2$, the reactant concentration, temperature, medium pH value and reaction time play important roles to control the morphology and sizes of copper sulfide nanocrystals. Figure 4 shows typical SEM images of CuS crystals for different C_R. While the C_R = 0.5, 1, 2, 3, 3.2 and 4 at 160 °C for 8 h, respectively, the size and morphology of copper sulfide nanocrystals were quite different. The shapes of copper

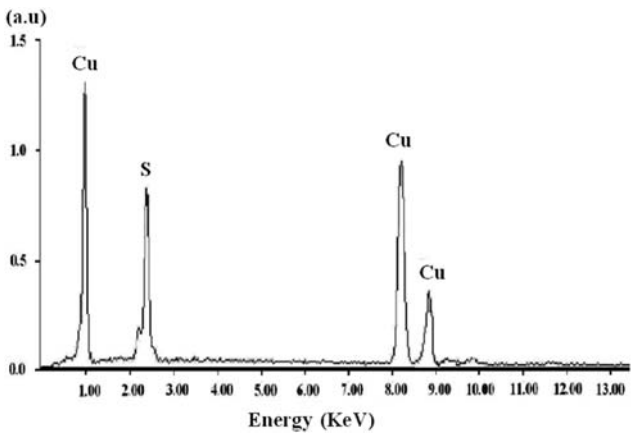

Fig. 2 EDX spectrum of as-prepared copper sulfide nanoflowers

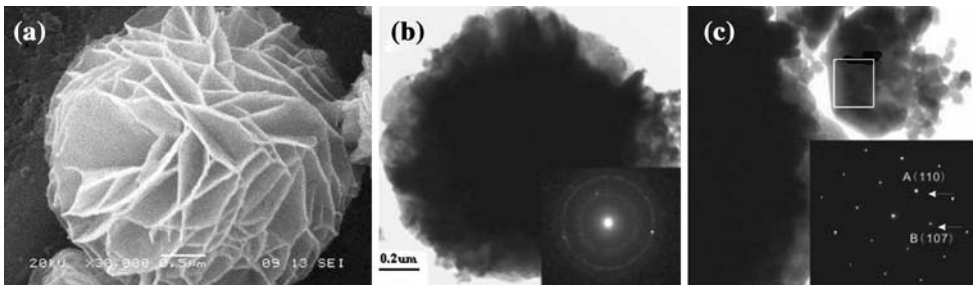

Fig. 3 SEM, TEM and SAED images of as-prepared copper sulfide products with 3D flower-shape. (**a**) SEM; (**b**) TEM; (**c**) TEM and SAED

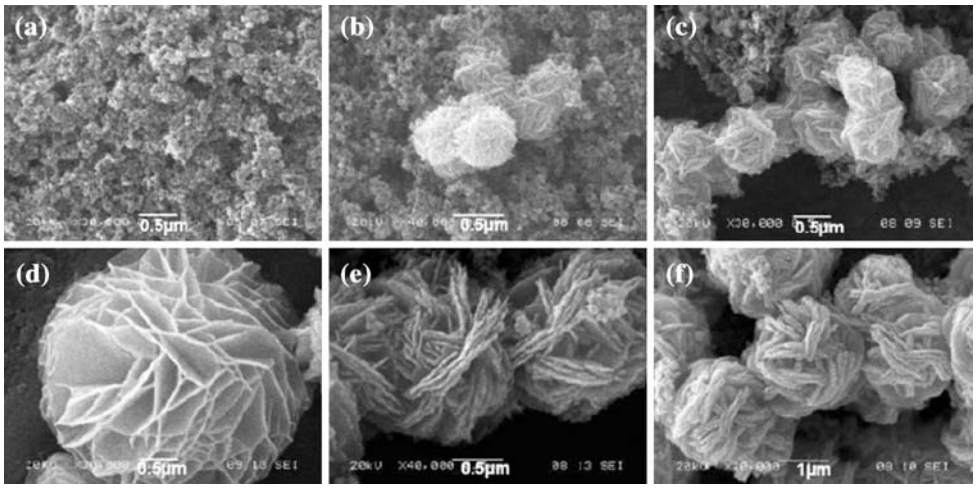

Fig. 4 SEM images of as-prepared copper sulfide products of different proportion C_R. (**a**) 0.5; (**b**) 1; (**c**) 2; (**d**) 3; (**e**) 3.2; (**f**) 4

sulfide crystals were changed from particle to flower shape gradually. Flower morphology of copper sulfide nanocrystals was formed at the $C_R \geq 3$. However, perfect CuS nanocrystals with 3D flower-shape was obtained at $C_R = 3$. Figure 5 shows typical SEM images of different initial concentration of reactant with $C_R = 3$ at 160 °C for 8 h. The different shapes of CuS crystals were formed at different initial reactant concentrations. Only Fig. 5c shows perfect 3D flower shape at 0.05 mol/L $Cu(ac)_2$.

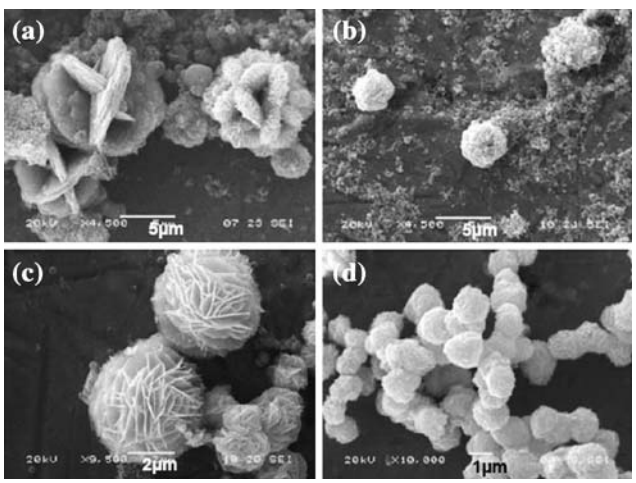

Fig. 5 SEM images of as-prepared copper sulfide products of different concentrations $Cu(ac)_2$ with $C_R = 3$ at 160 °C for 8 h: (**a**) 0.25 mol/L; (**b**) 0.10 mol/L; (**c**) 0.05 mol/L; (**d**) 0.025 mol/L

The representative SEM images of the samples obtained from different medium pH value with $C_R = 3$ at 160 °C for 8 h are shown in Fig. 6. The perfect CuS nanocrystal with 3D flower-shape was largely dependent on medium pH values. CuS particles or dollops were found at pH = 2, the conglobation of CuS particles with diameter of 22 um–10 um were produced at pH = 3, rulelessparticles were found at pH = 8. Only medium pH with 4 was in favor of ideal 3D flower shape formation of CuS nanocrystals. However, the XRD patterns recorded for these samples indicate that they are hexagonal phase.

In addition, the morphologies of CuS nanocrystals were sensitive to solvothermal temperature. The reactions at $C_R = 3$ were carried out at different temperatures, i.e., 150, 158, 160, 162 and 170 °C. Flower morphology of CuS nanocrystals was obtained at 158–162 °C for 8 h (data not shown), but perfect flower morphology was produced only at 160 °C. Thus ideal CuS nanocrystals with three-dimensional flower-shape were obtained at temperatures controlled strictly.

To understand the possible formation mechanism of the copper sulfide nanocrystals, the growth process of the nanocrystals was monitored by SEM and FTIR. The SEM images of the samples obtained after the reaction for 1, 1.5,

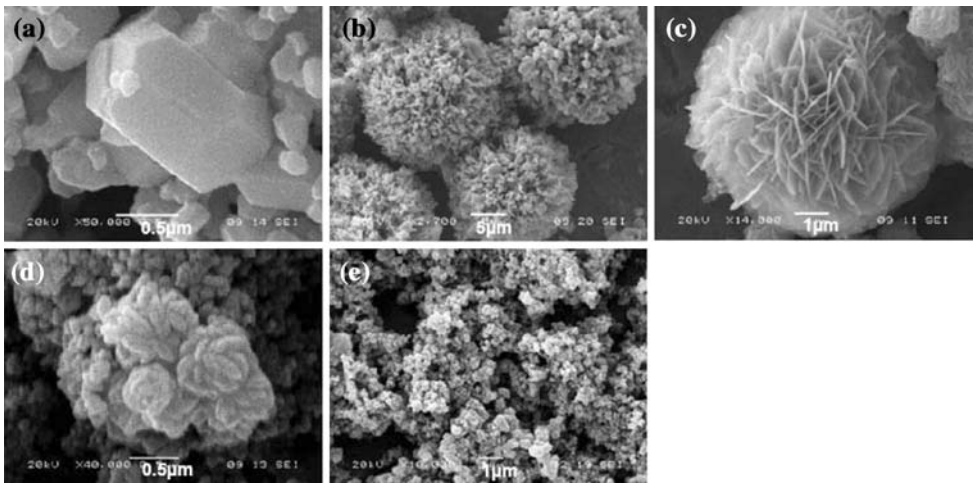

Fig. 6 SEM images of as-prepared copper sulfide products of different acidity. (**a**) pH = 2; (**b**) pH = 3; (**c**) pH = 4; (**d**) pH = 6; (**e**) pH = 8

1.75, 2 and 8 h at 160 °C are shown in Fig. 7 and their FTIR spectra are shown in Fig. 8. These images clearly exhibit the evolution of CuS flower shape over the periods of reaction time. At first, the ruleless sticks crystal of Cu–Tu complex with total length ranging from 260 nm to 850 nm was formed at 1 h (Fig. 7a), then those ruleless sticks crystals were congregated (Fig. 7b). The characteristic IR spectrum of the product obtained for 1 h (Fig. 8b) is comparable with one of Tu. Because the γ_{N-H} absorption bands in the region 3,100–3,400 cm^{-1} and δ_{N-H} 1,618 cm^{-1} in the spectrum of Tu were not shifted to lower frequencies on the formation Cu–Tu complex, it is concluded that Cu to N bonds are not present and that the bonding must be between Cu and S atom. It can be seen from spectrum Fig. 8a, b that the $\gamma_{C=S}$ at 1,413 $cm^{-1}$and 730 $cm^{-1}$of Tu are shifted to low frequencies 1,396 cm^{-1} and 705 cm^{-1}, respectively in Cu–Tu complex. Similarly the C–N stretching vibration at 1,084 cm^{-1} is shifted to higher frequency 1,108 cm^{-1}. This also shows that binding of Cu with Tu is through S [30, 31]. When the reaction proceed for 1.75 h, the similarly flower with diameter of about 0.8 μm was formed (Fig. 7c). The basic flower shape with diameter of about 1 μm was produced for 2 h (Fig. 7d). Continuously increasing the reaction time for ~8 h, perfect flower shape with diameter of ~2.5 um was fabricated (Fig. 7e). Meanwhile, the IR spectrum of the products prepared for 1.75, 2 and 8 h (Fig. 8c) shows a strong absorption in main IR field and presence of any impure composition was not observed. This result is supported by spectra of XRD and EDX.

Morphology and sizes control of CuS nanocrystals are accomplished by carefully controlling nanocrystal growth parameters such as reactant molar ratio (C_R), the reactant concentration, temperature, medium pH value and reaction time. The results suggest that the particle sizes and their shape depend on the nucleation rate, the growth rate and the growth habit of crystals. The nucleation rate and the growth rate of CuS nanocrystals with 3D flower-shape were well controlled by growth parameters in the present system.

On the basis of the above results, it could be believed that the formation of ideal flower morphology of CuS

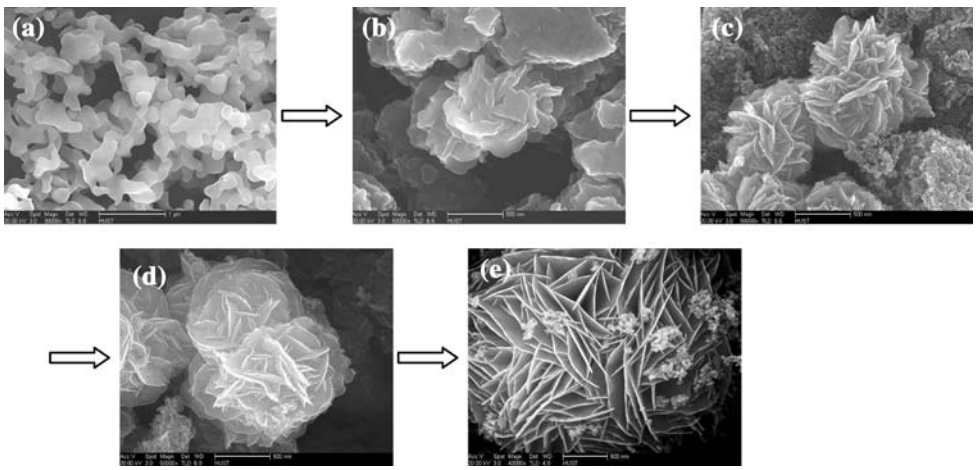

Fig. 7 SEM images of as-prepared copper sulfide products of different times. (**a**) 1 h; (**b**) 1.5 h; (**c**) 1.75 h; (**d**) 2 h; (**e**) 8 h

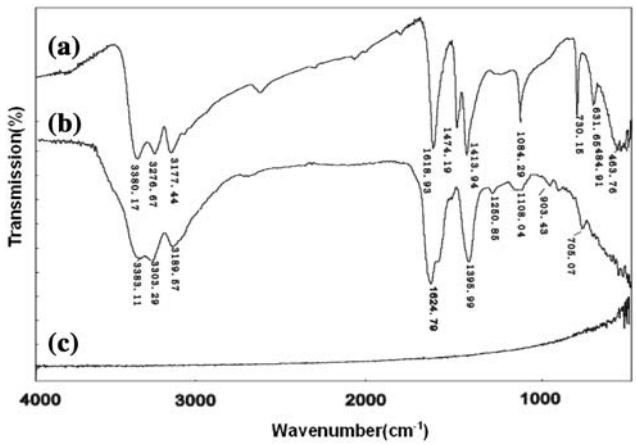

Fig. 8 IR spectra of as-prepared copper sulfide products. (**a**) thiourea; (**b**) 1 h; (**c**) 8 h

nanocrystals had followed a thermolysis of Cu–Tu precursor congeries and a ripening process of the crystals. One the one hand, as copper ions prefer square coordination with cit, the resulting extended chains can be connected into 2D layers through the coordination of hydroxyl ions to dz 2 orbitals of copper atoms. Thiourea molecules got attached with the cation $Cu(cit)_2^{2+}$ as start materials with plane structure which easily leads to the formation of resembled morphology of nanoparticle [32]. On the other hand, the hexagonal crystal nucleus of CuS are produced by a thermolysis of Cu–Tu precursor congeries. Further increasing reaction time, the thermodynamic regime governs the growth process and Cu–Tu complex continuously supply monomers on the [107] faces with low surface energy, and therefore promote the growth in the [107] direction of a flat structure. Hence, CuS nanosheets along the [107] plane [19] can readily intermesh each other to form a 3D flower-shape of CuS nanocrystals along with process of Ostwald.

The reaction mechanisms involved are:

$$Cu^{2+} + 2Cit \rightarrow [Cu(Cit)_2]^{2+} \quad (1)$$

$$NH_2CSNH_2 + 2H_2O \rightarrow 2NH_3 + CO_2 + H_2S \quad (2)$$

$$[Cu(Cit)_2]^{2+} + H_2S \rightarrow CuS + 2H^+ + 2Cit \quad (3)$$

$$nCuS \rightarrow [CuS]n \quad (4)$$

The optical properties of as-prepared CuS nanocrystals at room temperature were studied and were shown in

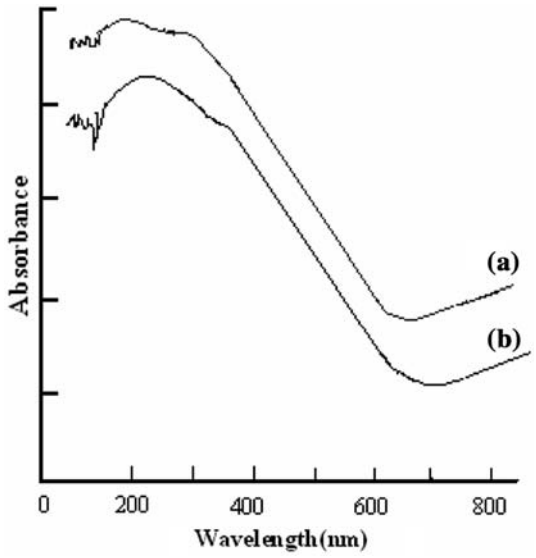

Fig. 9 UV–vis spectrum of copper sulfide nanocrystals (**a**) and bulk copper sulfide (**b**)

Fig. 9a. The UV–vis absorption spectrum of 3D-flower-shaped of CuS nanocrystals exhibits a well-defined absorption feature at 224 nm. This is considerably blue-shifted relative to the bulk value of 245 nm (Fig. 9b).

Conclusions

CuS nanocrystals with 3D flower-shape and hexagonal phase were synthesized via simple and free-template solvothermal method at low temperature. The CuS nanocrystals with 3D flower-shape were formed with a mass of nanosheets of interlacing arrangement. Moreover, the size and morphology of as-prepared products could be controlled by domination of reaction condition, including the molar ratio and concentration of reactant, reaction temperature, medium pH value, solvothermal reaction time.

Acknowledgments We thank the faculties from the Analysis and Test Center of Huazhong University of Science and Technology and Center for Electron of Microscopy of Wuhan University for the technical assistance on characterization.

References

1. Chen X, Nazzal A, Goorskey D, Xiao M (2001) J Phys Rev B 64:245304
2. Xin ZL, Jian BX (2002) J Phys Rev B 66:115316
3. Li M, Schnablegger H, Mann S (1999) Nature 402:393
4. Rodriguez JA, Jirsak T, Dvorak J, Sambasivan S, Fischer D (2000) J Phys Chem B 104:319
5. Huang MH, Mao S, Feick H, Yan H, Wu Y, Kind H, Weber E, Russo R, Yang P (2001) Science 292:1897
6. Mann S, Ozin GA (1996) Nature 382:313

7. Yang H, Coombs N, Ozin GA (1997) Nature 386:692
8. Ahmadi TS, Wang ZL, Green TC, Henglein A, ElSayed MA (1996) Science 272:1924
9. Lindroos S, Arnold A, Leskela M (2000) J Appl Surf Sci 158:75
10. Erokhina S, Erokhin V, Nicolini C (2003) J Langmuir 19:766
11. Reijnen L, Meester B, Goossens A, Schoonman J (2003) J Chem Vap Deposition 9:15
12. Sÿetkus A, Galdikas A, Mironas A, Sÿimkiene I, Ancutiene I, Janickis V, Kaciulis S, Mattogno G, Ingo MG (2001) J Thin Solid Films 391:275
13. Blachnik R, Muller A (2000) J Thermochim Acta 361:31
14. Parkin P (1996) J Chem Soc Rev 25:199
15. Yi HC, Moore JJ (1990) J Mater Sci 25:1159
16. Lu J, Zhao Y, Chen N, Xie Y (2003) J Chem Lett 32:30
17. Larsen TH, Sigman M, Ghezelbash A, Doty RC, Korgel BA (2003) J Am Chem Soc 125:5638
18. Dong X, Potter D, Erkey C (2002) J Ind Eng Chem Res 41:4489
19. Zhang P, Gao L (2003) J Mater Chem 13:2007
20. Xu CQ, Zhang ZC, Ye Q, Liu X (2003) J Chem Lett 32:198
21. Liao XH, Chen NY, Xu S, Yang SB, Zhu JJ (2003) J Cryst Growth 252:593
22. Lu Q, Gao F, Zhao D (2002) J Nano Lett 2:725
23. Chen X, Wang Z, Wang X, Zhang R, Liu X, Lin W, Qian YJ (2004) J Cryst Growth 263:570
24. Wang C, Tang K, Yang Q, Bin H, Shen G, Qian Y (2001) J Chem Lett 30:494
25. Gorai S, Ganguli D, Chaudhuri S (2005) J Cryst Growth Des 3:876
26. Ni Y, Liu H, Wang F, Yin G, Hong J, Ma X, Xu Z (2003) J Appl Phys A 10:1007
27. Qin AM, Fang YP, Ou HD, Liu HQ, Su CY (2005) J Cryst Growth Des 3:856
28. Peng ZA, Peng X (2001) J Am Chem Soc 123:1389
29. Joo J, Na HB, Yu T, Yu JH, Kim YW, Wu F, Zhang JZ, Hyeon T (2003) J Am Chem Soc 125:11100
30. Angelimary PA, Dhanuskodi S (2001) J Cryst Res Technol 36:1231
31. Yang J, Zeng JH, Yu SH, Yang L, Zhang YH, Qian YT (2000) J Chem Mater 12:2924
32. Wells AF (1983) Structural inorganic chemistry, 5th edn. Clarendon Press, Oxford, p 1113